ISSN 1330-3651 (Print), ISSN 1848-6339 (Online) https://doi.org/10.17559/TV-20231201001164
Original scientific paper

CFD Analysis of Smoke Extraction in High-Altitude Highway Tunnel Fires with Vertical Shafts

Xiaohua JIN*, Zhihao LIN, Shunheng HUA, Xinru TONG, Lingbo ZHANG, Jiankun GONG, Zhenzhen MU

Abstract: This research aimed to study the impact of different altitudes on the flue gas temperature and thermal stratification in the highway tunnel with a vertical shaft, by establishing a full-sized tunnel model using the numerical simulation software Fire Dynamics Simulator (FDS). Simulation experimental results were analyzed and it was found: first, with the same heat release power of fire source, the vertical, transverse and roof temperatures of both fire source and non-fire source sections in the tunnel all increased to a certain extent along with the increase of altitude; second, the vertical, transverse and roof temperatures of the tunnel all increased with the increased heat release rate of fire source at the same altitude, and the temperature of the fire source section was higher than that of the non-fire source section as a whole; third, the average temperature and stratification intensity of vertical flue gas in both sections showed an increasing trend with the increase of altitude, indicating that the intensity of flue gas thermal stratification at high altitude was greater than that at low altitude, because a large amount of flue gas accumulated in the upper tunnel and led to the increase of the roof flue gas temperature at high altitude.

Keywords: altitude; flue gas temperature; flue gas thermal stratification; tunnel fire; vertical shaft smoke extraction

1 INTRODUCTION

With the steady progress of the Belt and Road Initiative and the western development strategy in China, the domestic highway and railway transportation construction has gradually extended to the central and western regions, which involves a large number of tunnel construction, including endless high-altitude tunnels, due to the complex topography in those regions. According to the Statistical Bulletin on the Transportation Industry Development in 2021, the total length of highway tunnels has increased by 2699.6 km compared with 2020 [1, 2]. The unique structural characteristics of highway tunnels limit the firefighting and rescue activities. For high-altitude tunnels, harsh environmental characteristics, such as low temperature, low pressure and oxygen content, pose a serious threat to the life and property safety of trapped people [3-5]. Therefore, efficient flue gas control and emission of the high-altitude tunnel fire not only has become an important research content in the tunnel safety management field [6-8], but also is an important work link in tunnel fire control design.

Many scholars have conducted a series of studies on the development characteristics of tunnel fire at different altitudes. Wieser et al. [9] studied the tunnel fire development trend within an altitude range of 400 m ~ 3000 m, based on a 6 m × 2.8 m × 2.1 m scaled highway tunnel experimental model. The experimental results showed that the environmental pressure and oxygen density gradually decreased along with the increase of altitude, which led to a gradual slowdown in the fire development speed. Yan et al. [10] studied the effects of high-altitude environmental pressure on the flue gas flow in vertical shafts in natural ventilation tunnel fire using the established FDS mathematical model. The results showed that the fire flue gas flow rate was relatively high at lower environmental pressure, because low-pressure environment caused high flue gas temperature. Ji et al. [11] established a 150 m × 10 m × 5 m full-sized highway tunnel mathematical model using FDS and explored the influence rule of environmental pressure change on the flue gas movement and temperature distribution in a tunnel fire through experiment. It was found that the reduced environmental pressure led to the reduction of air density and the weakening of air entrainment, which caused the increase of vertical flue gas temperature. Tan et al. [12] studied the effects of environmental pressure on the efficiency of mechanical smoke extraction system in a highway tunnel fire, based on the established 70 m × 10 m × 5 m full-sized theoretical model. The simulation results showed that the decreased environmental pressure led to the increasing thickness trend of the flue gas layer and the flue gas spread speed, and the critical exhaust rate maximized the smoke extraction efficiency. Ji et al. [13] established a 130 m × 10 m × 5 m highway tunnel mathematical model using FDS, and studied the flue gas movement rule and temperature distribution rule in inclined tunnel fire under different environmental pressures. The results showed that the mass velocity of air and flue gas entrained in tunnel smoke extraction decreased with the decrease of environmental pressure, while the flue gas temperature increased with the decrease of environmental pressure, which provided a design reference for the smoke control and extraction system of high-altitude tunnel fire. Ji et al. [14] established a 150 m × 10 m × 5 m full-sized high-altitude highway tunnel theoretical model, based on the actual size of the highway tunnel, and studied the impact of environmental pressure change within the range of 50 kPa ~ 100 kPa on the flue gas flow. It was found that the flue gas mass velocity also showed a decreasing trend along with the decrease of environmental pressure. Based on the analysis of simulation results, a quantitative model of the average flue gas mass flow rate in the one-dimensional diffusion stage was proposed. Yan et al. [15] studied the influence of environmental pressure on the critical wind speed and the reverse flue gas flow length of a vertical ventilation tunnel fire, by utilizing the established 200 m × 10.8 m × 7.2 m full-sized highway tunnel theoretical model. It was found that the critical wind speed increased with the increase of the heat release rate of fire source under different environmental pressures, and remained unchanged after the heat release rate increased to a certain extent. Xu et al. [16] studied the influence rule of

environmental pressure and vertical ventilation speed on the flue gas layer stability and the maximum roof temperature in the tunnel, based on the established 160 m × 10 m × 8 m full-sized tunnel model. The results showed that the flue gas flow rate was affected by the vertical ventilation speed and the environmental pressure. It was found that the maximum roof flue gas temperature was negatively correlated with the vertical wind speed and the environmental pressure. In addition, a model was developed to predict the maximum roof flue gas temperature in the tunnel with different heat release rates of fire source, vertical velocities and environmental pressures. Yao et al. [17] used FDS to model a 350 m × 5 m × 5 m full-size road tunnel to investigate the effect of ambient pressure on the movement of smoke in a fire tunnel, and found that the thickness of smoke downstream of the fire source increases with the increase of ambient pressure and longitudinal wind speed when the rate of heat release from the fire source is certain. He et al. [18] used FDS to build a full-size stairwell and investigated the effects of ambient pressure and heat release rate on the flow of flue gas in the stairwell, and found that the mass flow rate of the air entering the stairwell increased as the ambient pressure increased. Zhang et al. [19] used FDS to build a 280 m × 5 m × 5 m full-size sloped tunnel to investigate the effects of ambient pressure and tunnel slope on the temperature distribution and smoke spread of fire in a full-size sloped tunnel, and the results showed that the velocity of the inlet airflow decreases with the increase of ambient pressure. Chen et al. [20] established a reduced-size T-bifurcation tunnel to investigate the effect of the longitudinal position of the fire source on the critical tunnel wind speed, and concluded that when the position of the fire source is located in the T-intersection or in the upstream of the intersection, the critical tunnel wind speed increases with the increase of the longitudinal position L of the tunnel fire source, and when the fire source is located in the downstream of the intersection, the critical wind speed does not change with the change of the position of the fire source.

At present, most of the scholars based on experimental and numerical simulation methods have studied the effect of environmental pressure on the mechanical smoke exhaust efficiency of road tunnel fire and the thickness of the smoke layer and the speed of smoke spread in the tunnel. Currently there are fewer studies on the effect of ambient pressure on the spread of fire in shaft road tunnels. This research studied the influence rule of different altitudes and fire source power on fire development characteristics in the highway tunnel with a vertical shaft using FDS, which provided certain technical support for smoke control and extraction in high-altitude highway tunnels with vertical shafts.

2 RESEARCH MODEL

2.1 Modeling

A highway tunnel model with a vertical shaft, with the dimensions of 120 m × 10 m × 5 m, was established in this study based on FDS software. The tunnel's center point was the origin of coordinates, and the vehicle that caught fire was located on the tunnel centerline. Length and width of the fire source were 6 m and 2 m, with n-heptane as the fuel. Stable fire was used, and the fire source power did not change over time. The vertical shaft, with the dimensions of 2 m × 2 m × 5 m, was located 20 m to the right of the fire source center point. The vehicles passing through tunnel highways were generally cars, trucks and buses, with 5 MW, 10 MW and 20 MW as their fire source power, respectively. The tunnel's initial temperature was set to 20 °C, and all tunnel walls were set to be "concrete". Entrance and exit at both ends of the tunnel and the vertical shaft exit were set to be "open", i.e. connected to the external environment. The model is shown in Fig. 1.

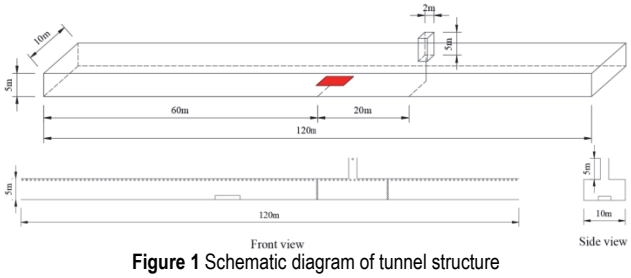

Figure 1 Schematic diagram of tunnel structure

2.2 Measuring Point Arrangement and Simulated Working Conditions

In this study, 120 temperature measuring points were evenly arranged every 1m along the tunnel centerline from 0.1 m below the roof. Temperature measuring point and carbon monoxide (CO) concentration measuring point were arranged vertically at 12 m and 26 m downstream of the fire source, with a spacing distance of 0.2 m between them. Temperature measuring points were arranged horizontally with a spacing distance of 0.5 m, as shown in Fig. 1. According to the design specifications [21], the safe evacuation standards were set as follows: (1) the flue gas temperature at 2 m of human eye characteristic height was below 60 ℃; (2) the roof temperature shall not exceed 180 ℃. Characteristics of fire combustion and flue gas movement in the highway tunnel with a vertical shaft were studied by mainly changing the tunnel altitude. The simulated working conditions are shown in Tab. 1.

Table 1 Simulated working condition setting

No.	Fire source power / MW	Altitude / m
1 - 5	5	0/950/1,850/2,750/4,200
6 - 10	10	0/950/1,850/2,750/4,200
11 - 15	20	0/950/1,850/2,750/4,200

2.3 Grid Partition

As a three-dimensional fire fluid dynamics computation simulation software, FDS solved the Naviere-Stokes equation of low-speed thermal drive, thus providing strong support for the simulation study of the fire development trends of various buildings and the flue gas spread characteristics. McGrattan et al. [22] pointed out through independent grid size verification experiments that the results of the fluid viscous stress model were accurate when the ratio of the fire source characteristic diameter D^* to the grid size δx was between 4 and 16. The calculation formula of the fire source characteristic diameter length D^* was given in Eq. (1).

$$D^*=\left(\frac{Q}{\rho_\infty c_p T_\infty g^{1/2}}\right)^{2/5} \quad (1)$$

where, D^* is the fire source characteristic diameter length (m), Q is the fire source power (KW), c_p is the specific heat at constant pressure, with KJ/(kg·K) as the unit, ρ_∞ is the environmental density (kg/m^3), T_∞ is the environment temperature (K), and g is the gravitational acceleration (m/s^3).

Different grid sizes were simulated and verified before simulation in order to establish qualified grid sizes. Four different grid sizes, namely, 0.167 m, 0.2 m, 0.333 m, and 0.5 m, were selected for simulation. According to Eq. (1), the smaller the fire source combustion power, the smaller the grid size. Therefore, the minimum fire source power of 5 MW was taken as an example to observe the temperature and CO concentration change in the vertical direction at 13 m downstream of the fire source center point with different grids. The change over time is shown in Fig. 2.

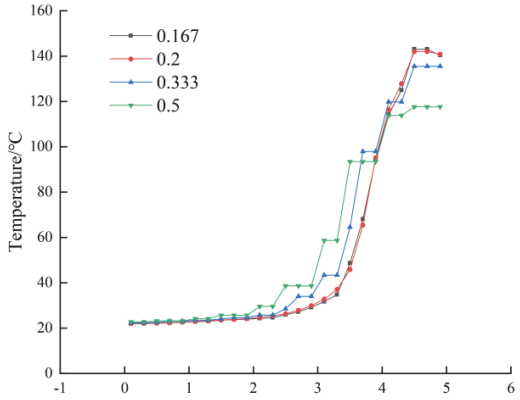

(a) Vertical temperature

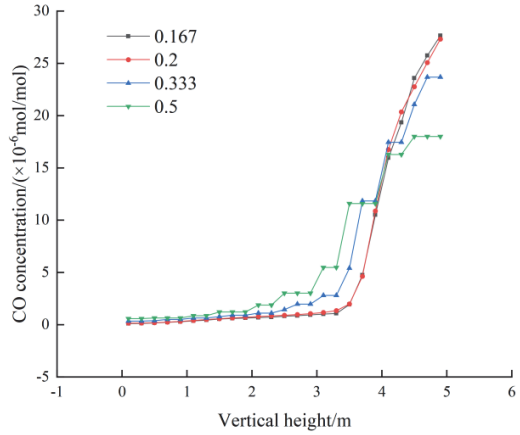

(b) Vertical CO concentration

Figure 2 Grid independence verification

It can be seen from the figure that there is no significant difference in temperature and CO concentration curves when the grid size is less than 0.5 and the computer used in this simulation has a CPU of 20 cores. Therefore, a grid size of 0.333 m and the simulation time of 360 s were used in this simulation, by taking into consideration the simulation accuracy and operation performance of the computer.

3 RESULTS AND DISCUSSION

3.1 Impact of Altitude on Vertical Flue Gas Temperature in the Tunnel

Vertical temperature in fire source and non-fire source sections of the tunnel was studied in order to discuss the impact of altitude on temperature distribution. Fig. 3 and Fig. 4 are the vertical temperature distribution maps of both sections.

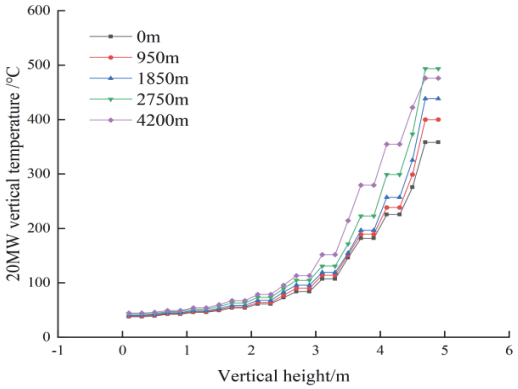

Figure 3 20 MW vertical temperature of fire source section

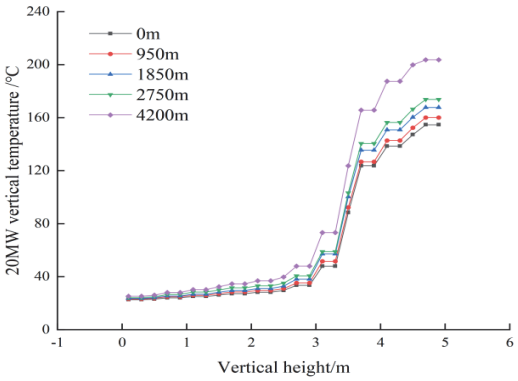

Figure 4 20 MW vertical temperature of non-fire source section

It can be seen from the figures that the vertical temperature of both sections increases with the increase of the tunnel height with the same fire source power and altitude, and the overall vertical temperature of both sections in high-altitude areas is higher than that in low-altitude areas. The highest vertical temperature of the fire source section at 4200 m above sea level was 390 ℃, which was 82 ℃ higher than that at 0 m above sea level, indicating that the high-altitude fire temperature posed greater harm to tunnel safety with the same fire source power. Therefore, the fire control requirements in high-altitude areas were higher. When the height was greater than 3.4 m, the vertical temperature gradient of both sections significantly changed, indicating that the 3.4 m height reached the flue gas layer height. According to related specifications [23], the standard of setting safe evacuation was that the flue gas temperature at 2 m of human eye characteristic height was below 60 ℃. As shown in Fig. 3 and Fig. 4, the temperatures at 2 m of human eye characteristic height in the fire source section at different altitudes are greater than 60 ℃, and those in the non-fire source section are less than 60 ℃ when the fire source power is 20 MW, which meets the required safe evacuation standard, indicating that the chimney effect of

the vertical shaft has effectively reduced the temperature at the human eye characteristic height in the tunnel, thus providing more rescue time for tunnel fire escape.

Fig. 5 shows the vertical temperature distribution of fire source and non-fire source sections at an altitude of 4200 m with 20 MW fire source power. It can be seen from the figure that the vertical temperature of the fire source section is higher than that of the non-fire source section as a whole with the same altitude and fire source power, and the vertical temperature change curves of both sections tend to be consistent, showing the "S" shape. The vertical temperature of both sections changed slowly near the ground, rose sharply after being 3.4 m away from the ground, and rose gradually after being 1m away from the roof. When a tunnel fire occurred, the vertical direction of the tunnel was divided into three parts, namely, the cold air layer, the mixed layer, and the flue gas layer. The roof was located near the flue gas layer. The ground was located near the cold air layer. The mixed layer was located between the two layers. Therefore, the temperature near the roof was relatively high and the vertical flue gas temperature gradient was gentle; due to being far away from the flue gas layer, the amount of flue gas was very small and the temperature was low in the cold air layer and the vertical flue gas temperature fluctuation was relatively small; however, the entrainment and heat exchange of fresh cold air and high-temperature flue gas in the mixed layer led to relatively large vertical temperature gradient.

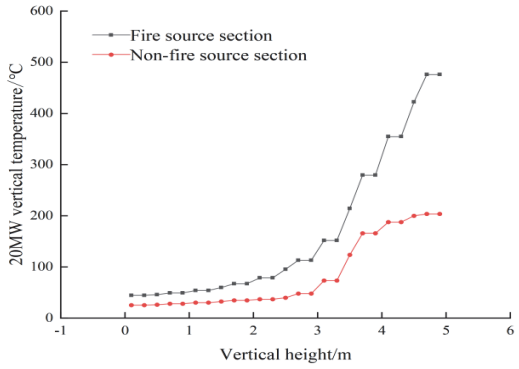

Figure 5 Vertical temperature at an altitude of 4200 m

3.2 Impact of Altitude on Transverse Flue Gas Temperature in the Tunnel

Fig. 6 and Fig. 7 show the transverse temperature distribution of fire source and non-fire source sections with 20 MW fire source power, respectively.

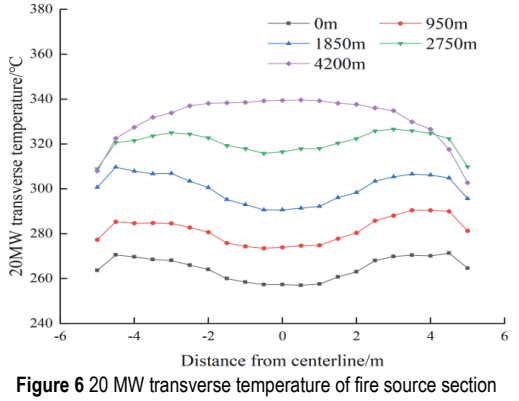

Figure 6 20 MW transverse temperature of fire source section

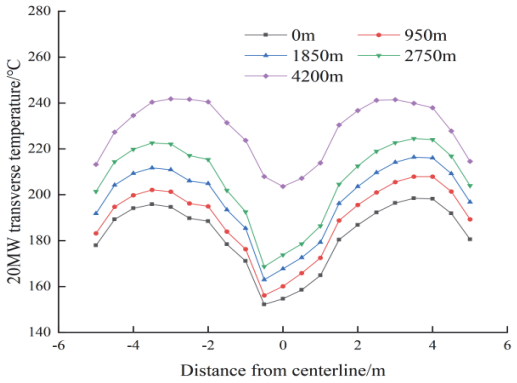

Figure 7 20 MW transverse temperature of non-fire source section

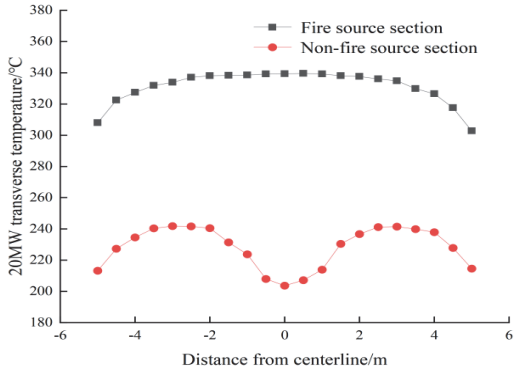

Figure 8 Transverse temperature at an altitude of 4200 m

It can be seen from the figures that the transverse temperature curve of both sections is in the "M" shape. In addition, the transverse temperature on the centerline of the fire source section is not much different from the temperature near the walls, while that of the non-fire section is significantly lower than the transverse temperature near the walls, because the vertical shaft is located on the centerline, which significantly reduces the transverse temperature near the centerline. The transverse temperature of both sections increased with the increase of altitude with the same fire source power, and the transverse temperature of the fire source section was higher than that of the non-fire source section as a whole. The highest transverse temperature of the fire source section at an altitude of 4200 m was 339.6 ℃, which was 97.7 ℃ higher than that (241.7 ℃) in the non-fire source section at an altitude of 0 m, indicating that the transverse temperature inside the tunnel was higher at high altitude, and caused greater harm to the tunnel structure. Fig. 8 shows the transverse temperature distribution of both sections at an altitude of 4200 m when the fire source power is 20 MW. It can be seen from the figure that the transverse temperature of the fire source section is significantly higher than that of the non-fire source section, and the transverse temperature difference near the centerline is greater, indicating that the chimney effect of the vertical shaft is good, which has taken away a large amount of high-temperature flue gas and effectively reduced the temperature in the tunnel.

3.3 Impact of Altitude on Vertical Flue Gas Temperature in the Tunnel

Fig. 9 shows the influence rule of altitude and fire

source power on the roof vertical temperature in the tunnel. As shown in the figure, the roof vertical temperature distribution presents a similar variation trend along with the distance change from the fire source, with different altitudes and fire source power. The roof vertical temperature change oscillates near the fire source center point, and the maximum value occurs. Then the roof vertical temperature rapidly decreases as the distance from the fire source center point gradually increases, reaches the minimum value at the vertical shaft position, and the temperature change gradually flattens out after the vertical shaft position because of heat exchange between flue gas and cold air and tunnel walls during the spread of flue gas, resulting in a decreasing temperature trend.

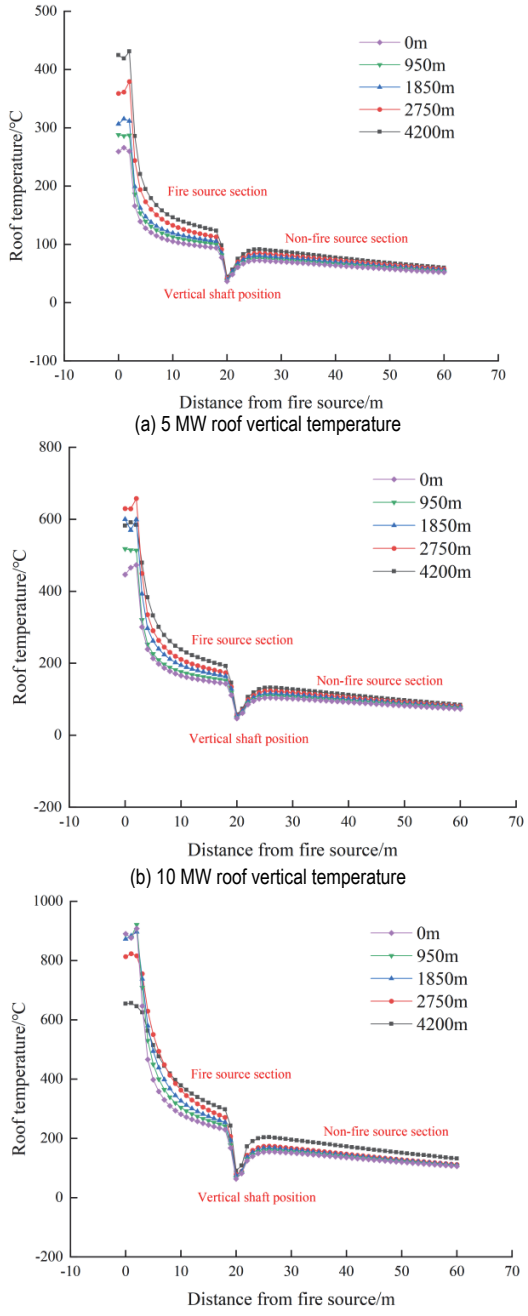

(a) 5 MW roof vertical temperature

(b) 10 MW roof vertical temperature

(c) 20 MW roof vertical temperature

Figure 9 Roof vertical temperature

However, the smoke outlet entrainment effect of the vertical shaft leads to the minimum roof vertical temperature at the vertical shaft position. As shown in the figure, at the non-fire source center point with different fire source power, the vertical roof temperature increases with the increase of altitude, because the altitude increase leads to the decrease of air density and flue gas entrainment capacity. When the altitude increases to 4200 m, the oxygen content in the air decreases by about 45% compared with that at sea level, resulting in a smaller decrease of flue gas temperature. As shown in Fig. 9, the roof flue gas temperature increases with the increase of the fire source power at an altitude of 4200 m; the highest roof vertical temperature increases by 224 ℃ with 20 MW fire source power compared with that with 5 MW fire source power.

3.4 Impact of Altitude on flue Gas Thermal Stratification in the Tunnel

The important factor affecting flue gas thermal stratification in the tunnel space was thermal buoyancy. Strang and Fernando [23] proposed the concept of buoyancy frequency regarding thermal stratification, which is the buoyancy change rate in the vertical direction:

$$N_{\mathrm{L}}=\left(-g\frac{\partial\rho_{\mathrm{i}}}{\partial z}/\rho_0\right)^{1/2}=\left(-gT_{\alpha}\frac{\partial\left(1/T\right)_{\mathrm{i}}}{\partial \mathrm{z}}\right)^{1/2} \tag{2}$$

where, N_{L} is the vertical buoyancy in the tunnel, ρ_{i} is the vertical density distribution in the tunnel, ρ_0 is the air density, T_{α} is the ambient temperature, and T_{i} is the vertical temperature distribution in the tunnel. With N_{L} as the maximum value of the vertical distribution in the tunnel, the more obvious the extreme value, the more obvious the thermal stratification intensity. This method was used to determine both the hot layer distribution and the flue gas layer height.

Eq. (3) was used to calculate the stratification intensity of the flue gas layer at different heights. It was simplified by using the vertical temperature change ΔT to represent buoyancy frequency in order to study the thermal stratification intensity in the tunnel:

$$\Delta T=T_{\mathrm{aver}}\cdot\frac{I_{\mathrm{s}}}{\Delta h^{*}} \tag{3}$$

where, T_{aver} is the average temperature of the tunnel cross-section, I_{s} is the flue gas stratification intensity, Δh^{*} is the dimensionless height difference, then the stratification strength I_{s} was given by Eq. (4):

$$I_{\mathrm{s}}=T_{\mathrm{c}}^{*}-T_{\mathrm{d}}^{*}=\frac{T_{\mathrm{c}}}{T_{\mathrm{aver}}}-\frac{T_{\mathrm{d}}}{T_{\mathrm{aver}}}=\frac{T_{\mathrm{c}}-T_{\mathrm{d}}}{1/n\sum_{1}^{\mathrm{n}}T_{\mathrm{i}}} \tag{4}$$

where, T_{c}^{*} and T_{d}^{*} are the highest and lowest vertical dimensionless temperatures of the tunnel cross-section, T_{c} is the highest vertical temperature of the cross-section, T_{d} is the lowest vertical temperature of the cross-section, n is the number of measuring points, T_{i} is the temperature of the measuring point, and Δh^{*} is the dimensionless height difference, which is the ratio of the height difference

between the highest and lowest temperatures T_c and T_d to the tunnel height H.

The vertical temperature rise of the tunnel cross-section determined the buoyancy frequency N_L because g and T_α in Eq. (3) were constants. When the average temperature T_{aver} of the tunnel cross-section and the dimensionless height difference Δh^* were constant values, it was calculated from the Eq. (3) that the vertical average temperature ΔT increased as the stratification strength increased, and from the Eq. (2) that the buoyancy value further increased, indicating an increase in the flue gas stratification intensity of the tunnel cross-section. Therefore, stratification intensity indirectly reflected the hot layer distribution of flue gas in the upper tunnel and the fresh air in the lower layer under certain conditions.

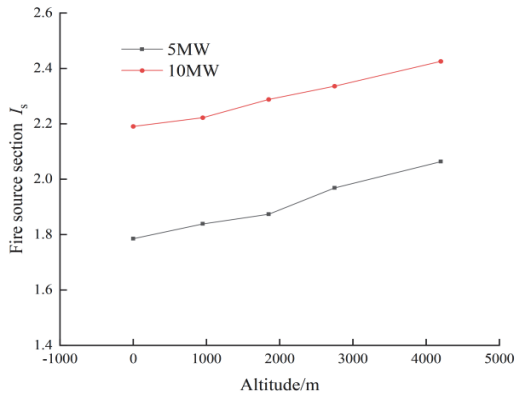

Figure 10 Fire source section I_s

The buoyancy frequency method was used in this study to determine the flue gas thermal stratification. The stratification intensity of fire source and non-fire source sections are shown in Fig. 10 and Fig. 11. It can be clearly seen from the figures that the stratification intensity increases significantly as the altitude increases, and the stratification intensity at different altitudes is the dimensionless temperature difference ($\Delta h^* = 0.95$) between the highest and lowest points of the tunnel cross-section. With the dimensionless height difference as a constant, as the altitude increased and the environmental pressure decreased, both the average temperature and the stratification intensity increased, and then the vertical temperature change ΔT also increased.

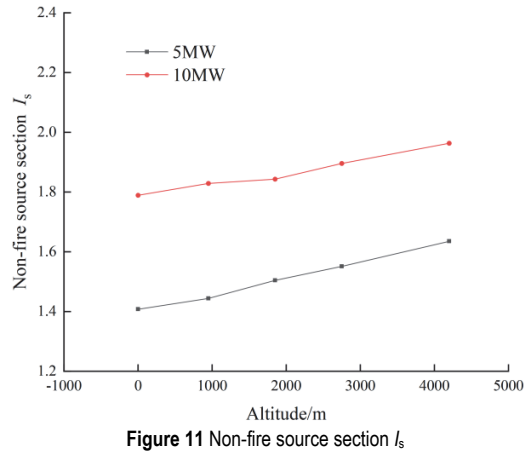

Figure 11 Non-fire source section I_s

As the altitude increased, the thermal stratification intensity in cross sections of both sections continuously increased because ΔT determined the buoyancy frequency. The increase of thermal stratification intensity indicated that the flow stability of flue gas and air in the cross sections of both sections strengthened. Therefore, it was more conducive to creating safe evacuation space in the highway tunnel in high-altitude areas than that in low-altitude ones, when a fire occurred in the tunnel. Under the premise of stable stratification of the flue gas layer, the larger vertical smoke extraction wind speed could be adopted in the high-altitude highway tunnel.

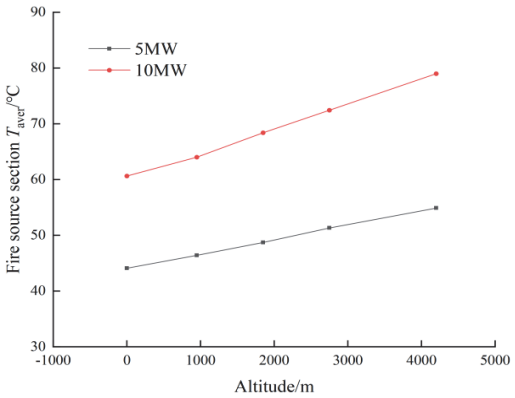

Figure 12 Fire source section T_{aver}

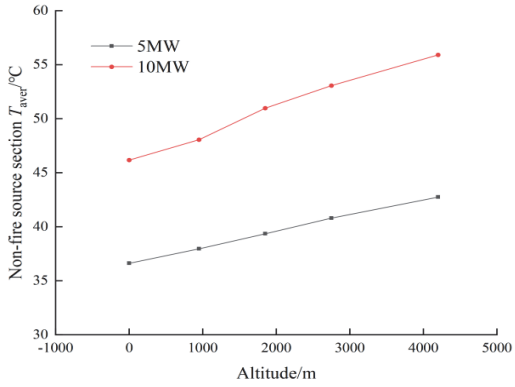

Figure 13 Non-fire source section T_{aver}

Fig. 12 and Fig. 13, respectively, show the change in the average temperature T_{aver} of the cross sections of both sections as the altitude changes. It can be seen from the figures that the average cross section temperature of both sections increases with the increase of the altitude and the fire source power in the tunnel.

When a tunnel fire occurred, the fire source generated a large amount of high-temperature flue gas, which moved upward under the action of thermal buoyancy, and began to move outward along the roof after rising to the roof. At the same time, the high-temperature flue gas exchanged heat with fresh air, which led to the decreased flue gas temperature and thermal buoyancy. When the flue gas reached a certain height, a neutral surface was formed between it and the air layer, and a flue gas layer was formed. Stability of the flue gas layer was the combined action result of thermal buoyancy and inertial force of the flue gas. The thermal buoyancy was beneficial for the flue gas thermal stratification. However, the inertial force enhanced the movement of high-temperature flue gas

towards the cold air layer, leading to chaos in the flue gas layer. The greater intensity of flue gas thermal stratification in high-altitude areas led to the decreased amount of entrained fresh cold air during the flue gas flow process, which reduced the heat exchange between flue gas and fresh cold air, and then increased the flue gas temperature and the thermal buoyancy, proving that the roof temperature in high-altitude areas was higher than that in low-altitude ones in the sections above.

3.5 ANOVA

Based on the data above, the detection data at 40 m downstream of the fire source was selected as the parameter for ANOVA, and the longitudinal temperature of the roof was taken as the index of analysis, and the ANOVA of orthogonal test was used to calculate and process the data above to obtain Tab. 2, which has determined the significance and reasonableness of the influence of the power of the fire source and the altitude of the fire source on the longitudinal temperature of the roof. As can be seen from Tab. 2, the *P*-values for both fire power and altitude are less than 0.05, indicating that both fire power and altitude have a significant effect on the longitudinal temperature of the ceiling.

Table 2 Temperature ANOVA table

Factor	*SS*	d*f*	*F*	*P*
Fire source power	15,20.74	2	266.79	0.0000000476
Altitude	1,014.73	4	8.95	0.004747872
	226.70	8		

4 CONCLUSION

The influence rule of altitude on smoke extraction of the vertical shaft in the highway tunnel was comprehensively analyzed based on FDS software, which obtained the change rule of vertical and transverse temperatures, vertical roof temperature, and flue gas thermal stratification of fire source and non-fire source sections. The following conclusions were drawn:

(1) With the same fire source power and altitude, the vertical temperature of both sections increased with the increase of tunnel height, and the overall vertical temperature of both sections in high-altitude areas was higher than that in low-altitude ones. The increase in vertical temperature at high altitude poses a great challenge to firefighting and rescue, and we need to raise the standard of firefighting and rescue when responding to high altitude fires.

(2) The transverse temperature curve of both sections showed the "M" shape. The transverse temperature on the centerline of the fire source section was not significantly different from the temperature near the walls, while that of the non-fire source section was significantly lower than the transverse temperature near the walls. With the same fire source power, the transverse temperature of both sections increased with the increase of altitude, and the transverse temperature of the fire source section was higher than that of the non-fire source section as a whole.

(3) With the same fire source power at different altitudes, the characteristic curves of roof temperature at different altitudes were consistent. The higher the altitude, the higher the roof temperature of both sections in the tunnel. With the same altitude, the greater the fire source power, the higher the roof temperature of both sections. Using analysis of variance (ANOVA), it was verified that fire power and altitude had a significant effect on roof temperature.

(4) As the altitude increased, the stratification intensity significantly increased, and the thermal stratification intensity in the cross sections of both sections continuously increased. The increased thermal stratification intensity indicated that the flow stability of flue gas and air in both sections strengthened. When a tunnel fire occurred, it was more conducive to creating safe evacuation space in the highway tunnel in high-altitude areas than that in low-altitude ones. Under the premise of stable stratification of the flue gas layer, the larger vertical smoke extraction wind speed could be adopted in the high-altitude highway tunnel.

The lack of full-scale real experiments in this study has some limitations, which can be followed up by real-scale experiments to investigate the effect of ambient pressure and heat release rate from the ignition source on road shaft tunnel fires to validate the simulation experiments.

5 REFERENCES

[1] 2021 Transport Industry Development Statistical Bulletin. https://xxgk.mot.gov.cn/2020/jigou/zhghs/202205/t20220524_3656659.html.

[2] 2020 Transport industry Development Statistical Bulletin. https://xxgk.mot.gov.cn/2020/jigou/zhghs/202105/t20210517_3593412.html.

[3] Feng, L. & Wang, Z. Y. (2007).CFDanlysis of fire ventilation in long highway tunnel with shaft. *Highway, 4*(4), 193-196.

[4] Hua, S. H., Tong, X. R., Qu, Q., & Xu, Y. (2023). Impact of high altitude low pressure environments on fire smoke propagation in highway tunnels. *International Journal of Heat and Technology, 41*(6), 1533-1542. https://doi.org/10.18280/ijht.41061

[5] Gong, J. K., Lin, Z. H., & Hua, S. H. (2022). Influence of ambient pressure over natural smoke ventilation in shaft tunnel fire. *International Journal of Safety and Security Engineering, 12*(2), 185-191. https://doi.org/10.18280/ijsse.120206

[6] Liu, B., Mao, J., Xi, Y., & Hu, J. (2021). Effects of altitude on smoke movement velocity and longitudinal temperature distribution in tunnel fires. *Tunnelling and Underground Space Technology, 112*, 103850. https://doi.org/10.1016/j.tust.2021.103850

[7] Li, H., Yao, W., Li, P., Zhou, Z., & Wang, J. (2017). Influence of high altitude on combustion efficiency and radiation fraction of hydrocarbon fires. *Heat Transfer Research, 48*(10), 865-875. https://doi.org/10.1615/HeatTransRes.2016010282

[8] Chen, X., Sun, Q., Wang, H., Xie, S., Liu, Y., & He, Y. (2019). The effect of pressure in cruise phase on the thermal runaway behaviors and smoke components. *2019 9th International Conference on Fire Science and Fire Protection Engineering*, 1-5. https://doi.org/10.1109/ICFSFPE48751.2019.9055814

[9] Wieser, D., Jauch, P., & Willi, U. (1997). The influence of high altitude on fire detector test fires. *Fire Safety Journal, 29*(2-3), 195-204. https://doi.org/10.1016/S0379-7112(96)00042-2

[10] Yan, G., Wang, M., Yu, L., Duan, R., & Xia, P. (2020). Effects of ambient pressure on smoke movement patterns in vertical shafts in tunnel fires with natural ventilation

systems. *Building Simulation, 13*, 931-941. https://doi.org/10.1007/s12273-020-0631-4

[11] Ji, J., Guo, F., Gao, Z., Zhu, J., & Sun, J. (2017). Numerical investigation on the effect of ambient pressure on smoke movement and temperature distribution in tunnel fires. *Applied Thermal Engineering, 118*, 663-669. https://doi.org/10.1016/j.applthermaleng.2017.03.026

[12] Tan, T., Yu, L., Ding, L., Gao, Z., & Ji, J. (2021). Numerical investigation on the effect of ambient pressure on mechanical smoke extraction efficiency in tunnel fires. *Fire Safety Journal, 120*, 103136. https://doi.org/10.1016/j.firesaf.2020.103136

[13] Ji, J., Wang, Z., Ding, L., Yu, L., Gao, Z., & Wan, H. (2019). Effects of ambient pressure on smoke movement and temperature distribution in inclined tunnel fires. *International Journal of Thermal Sciences, 145*, 106006. https://doi.org/10.1016/j.ijthermalsci.2019.106006

[14] Ji, J., Guo, F., Gao, Z., & Zhu, J. (2018). Effects of ambient pressure on transport characteristics of thermal-driven smoke flow in a tunnel. *International Journal of Thermal Sciences, 125*, 210-217. https://doi.org/10.1016/j.ijthermalsci.2017.11.027

[15] Yan, G., Wang, M., Yu, L., & Tian, Y. (2020). Effects of ambient pressure on the critical velocity and back-layering length in longitudinal ventilated tunnel fire. *Indoor and Built Environment, 29*(7), 1017-1027. https://doi.org/10.1177/1420326X19870313

[16] Xu, T., Tang, F., Xu, X., & He, Q. (2023). Impacts of ambient pressure on the stability of smoke layers and maximum smoke temperature under ceiling in ventilated tunnels. *Indoor and Built Environment, 32*(1), 85-97. https://doi.org/10.1177/1420326X211013080

[17] Yao, Y., Zhang, Y., Zhu, H, Han, Z., Zhang, S., & Zhang, X. (2023). Effects of ambient pressure on characteristics of smoke movement in tunnel fires. *Tunnelling and Underground Space Technology, 134*, 104981. https://doi.org/10.1016/j.tust.2023.104981

[18] He, J., Huang, X., Ning, X., Zhou, T., Wang, J., & Yuen, R. K. K. (2022). Modelling fire smoke dynamics in a stairwell of high-rise building: Effect of ambient pressure. *Case Studies in Thermal Engineering, 32*, 101907. https://doi.org/10.1016/j.csite.2022.101907

[19] Zhang, Y., Yao, Y., Ren, F., Zhu, H., Zhang, S., & Jiang, L. (2023). Effects of ambient pressure on smoke propagation in inclined tunnel fires under natural ventilation. *Environmental Science and Pollution Research, 30*(24), 65074-65085. https://doi.org/10.1007/s11356-023-26774-z

[20] Chen, C., Jiao, W., Zhang, Y., Shi, C., Lei, P., & Fan, C. (2023). Experimental investigation on the influence of longitudinal fire location on critical velocity in a T-shaped tunnel fire. *Tunnelling and Underground Space Technology, 134*, 104983. https://doi.org/10.1016/j.tust.2023.104983

[21] Code for Design on Rescue Engineering for Disaster Prevention and Evacuation of Railway Tunnel. TB 10020-2017.

[22] McGrattan, K. B., Forney, G. P., Floyd, J., Hostikka, S., & Prasad, K. (2005). *Fire Dynamics Simulator (version 4) - User's Guide*. Gaithersburg, MD, USA: US Department of Commerce, Technology Administration, National Institute of Standards and Technology.

[23] Strang, E. J. & Fernando, H. J. S. (2001). Entrainment and mixing in stratified shear flows. *Journal of Fluid Mechanics, 428*, 349-386. https://doi.org/10.1017/S0022112000002706

Contact information:

Xiaohua JIN
(Corresponding author)
School of Energy & Environment,
Zhongyuan University of Technology,
Zhengzhou 450007, China
E-mail: 6561@zut.edu.cn

Zhihao LIN
School of Emergency Management and Safety Engineering,
China University Mining and Technology Beijing,
Beijing 100083, China
E-mail: linzhihao428@163.com

Shunheng HUA
School of Energy & Environment,
Zhongyuan University of Technology,
Zhengzhou 450007, China
E-mail: 2021108209@zut.edu.cn

Xinru TONG
School of Energy & Environment,
Zhongyuan University of Technology,
Zhengzhou 450007, China
E-mail: 2022108372@zut.edu.cn

Lingbo ZHANG
School of Energy & Environment,
Zhongyuan University of Technology,
Zhengzhou 450007, China
E-mail: 2018108103@zut.edu.cn

Jiankun GONG
School of Energy & Environment,
Zhongyuan University of Technology,
Zhengzhou 450007, China
E-mail: 2019108141@zut.edu.cn

Zhenzhen MU
School of Energy & Environment,
Zhongyuan University of Technology,
Zhengzhou 450007, China
E-mail: 2021108289@zut.edu.cn